Extratropical Storms Fundamentally Shape the Maritime Surface Wind Climatology

Larry W. O'Neill[1], Ralph F. Milliff[2], and Dudley B. Chelton[1]

Oregon State University | College of Earth, Ocean, and Atmospheric Sciences

1: College of Earth, Ocean, and Atmospheric Sciences, Oregon State University, Corvallis, Oregon

2: Cooperative Institute for Research in Environmental Sciences, University of Colorado, Boulder, Colorado

(1) Abstract

Effects of synoptic weather variability on the climatological wind field over the global oceans has been unresolved due to lack of observations and difficulty clearly distinguishing storms from weaker background variability. This study reveals that synoptic weather variability imprints onto the climatological-mean wind field over the global oceans in a surprising manner. Mid-latitude storm events, defined as predominantly associated with extratropical cyclones, typically generate large-amplitude but short-lived convergent and cyclonic wind anomalies which are unambiguous from other processes. Using maritime surface vector winds from QuikSCAT satellite observations and ERA-Interim reanalysis, we show that removing fewer than 5% of the strongest convergent and cyclonic wind events removes nearly all time-mean convergence and cyclonic vorticity poleward of 50° latitude. Relatively few synoptic-scale weather events thus account for dynamically important features in the large-scale atmospheric circulation. Since the large-scale ocean response to wind forcing on the short timescales of synoptic weather events is weak, this result has important implications for understanding processes that drive the mid-latitude ocean circulation, which is generally thought to be driven by lower frequency wind variability. Climate model projections suggest that climate change will affect the location, frequency, and strength of synoptic-scale activity within the mid-latitude storm tracks. The derivative wind fields may aid assessment of how storms affect the large-scale atmospheric and oceanic circulation in climate model projections.

(2) Relative Amplitude of Synoptic Weather Disturbances in the derivative wind fields

The surface manifestation of synoptic-scale storms is evident in the surface derivative wind fields as large-amplitude but short-duration anomalies or "spikes" in time series extracted from these fields (Figure 1). These spikes represent convergent and cyclonic wind anomalies, consistent with earlier scatterometer-based analysis of surface wind stress curl and divergence variability (Milliff and Morzel 2001). Intense and intermittent convergent and cyclonic wind spikes punctuate a relatively tranquil background of much weaker divergent and anti-cyclonic flow. Divergence spike amplitudes of $5\times10^{-5}s^{-1}$ and wind stress curl spike amplitudes of $40\times10^{-7}N\ m^{-3}$ exceed background values by more than a factor of 5. In this analysis, we exploit extremes of the derivative vector wind fields as indicators of storm activity, rather than vector wind or wind speeds, since they clearly distinguish storm events from lower amplitude background variability.

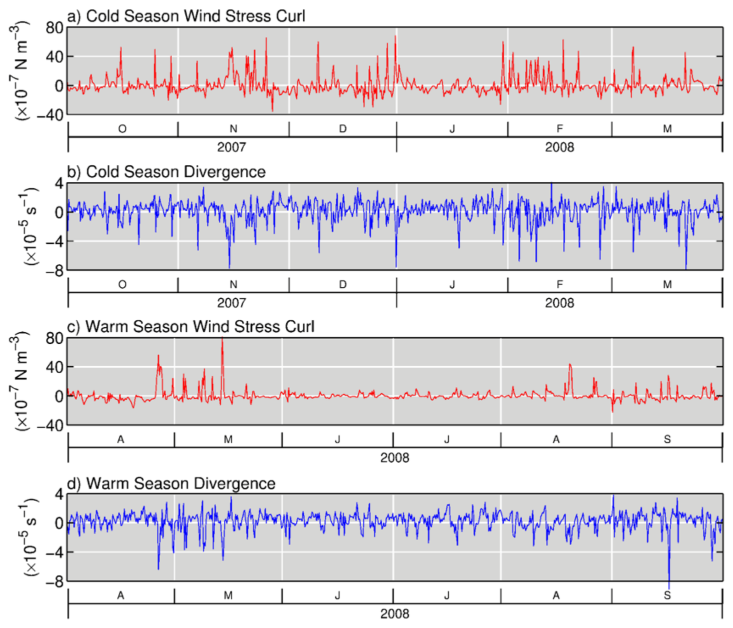

Figure 1: *Time series of the surface wind divergence and wind stress curl from the 6-hourly ERA-Interim reanalysis at Ocean Station Papa in the North Pacific during Oct 2007-Sept 2008.*

The PDFs for all 3 derivative wind quantities (Figure 3) are highly asymmetric in mid-latitudes since their skewness coefficients all have absolute magnitudes greater than 1. The PDFs are skewed toward convergent or cyclonic winds. *Extreme convergent and cyclonic wind events occur several times more often than divergent or anti-cyclonic winds.* This is consistent with the example time series in Figure 1 and maps in Figure 2, which suggests that typical wind conditions are divergent and anti-cyclonic and that large storm-induced convergent and cyclonic wind events interrupt this relatively tranquil background state.

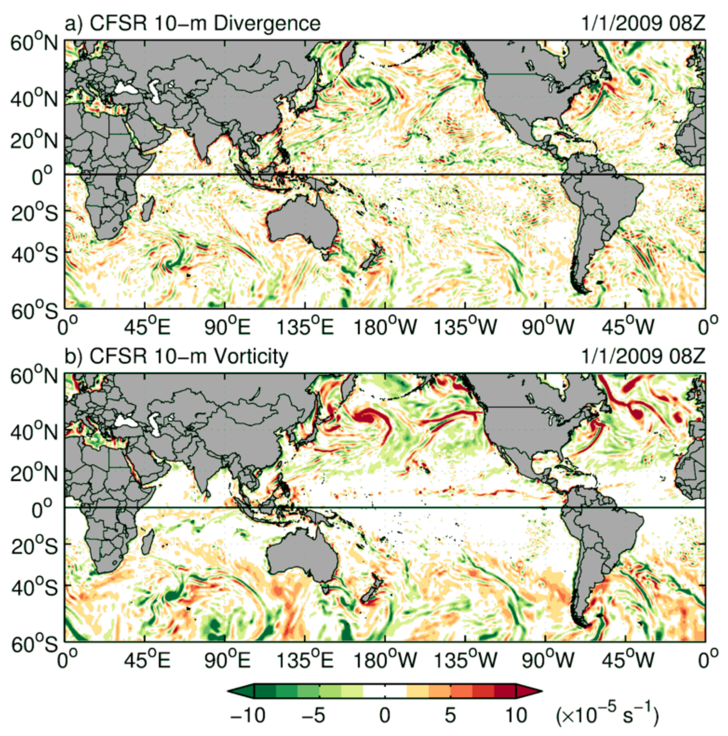

Figure 2: *Example maps of the instantaneous 10-m divergence and vorticity on 1/1/2009 from the CFSRv2 reanalysis. Extreme values more than an order of magnitude greater than the climatological time mean are prevalent throughout the mid-latitude storm tracks.*

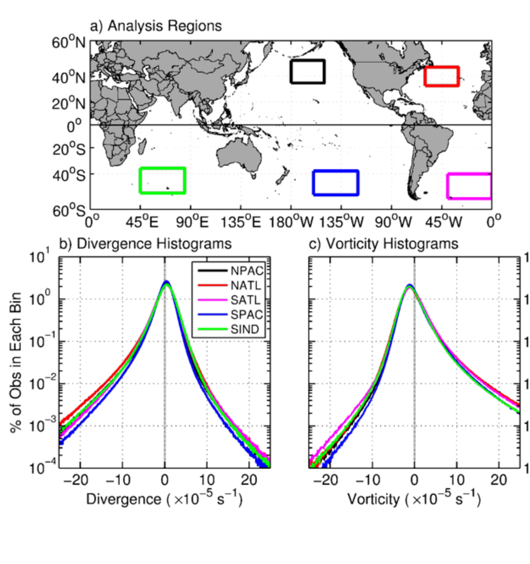

Figure 3: *Univariate probability distribution functions (PDFs) of the QuikSCAT divergence (b), vorticity (c), and wind stress curl (d) in the five regions color-coded in the map in panel (a). The vorticity and wind stress curl PDFs in panels (c) and (d) for the Southern Hemisphere regions have been multiplied by -1 to aid in comparison with the Northern Hemisphere regions.*

	Divergence $\times10^{-5}$ s^{-1}			Vorticity $\times10^{-5}$ s^{-1}			Wind Stress Curl $\times10^{-7}$ N m^{-3}		
	Mean	Median	Skewness	Mean	Median	Skewness	Mean	Median	Skewness
N. Pacific	0.0	0.4	−1.9	−0.1	−1.1	3.3	−0.1	−1.4	8.2
N. Atlantic	0.0	0.5	−1.9	−0.2	−1.2	3.4	−0.5	−1.6	9.5
S. Pacific	0.1	0.4	−1.7	0.3	1.2	−3.1	0.7	1.9	−6.2
S. Atlantic	0.0	0.4	−1.4	0.0	1.0	−2.8	0.1	1.7	−4.8
S. Indian	0.1	0.5	−1.7	0.4	1.2	−3.0	1.1	2.3	−5.0

(3) Effects of storm events on the climatological time-mean winds

Zonal and time mean profiles of divergence, vorticity, and wind stress curl are shown by the black curves in the top panels in Figure 4 from 10 years of QuikSCAT wind observations. The remaining curves are the profiles after removing divergence, vorticity, and wind stress curl anomalies with absolute values greater than *S* standard deviations (σ) from the mean (each color represents a different integer *S* according to the scale at the bottom). The percentages of observations removed by this simple extreme value filter are shown in the bottom panels according to the same color scale.

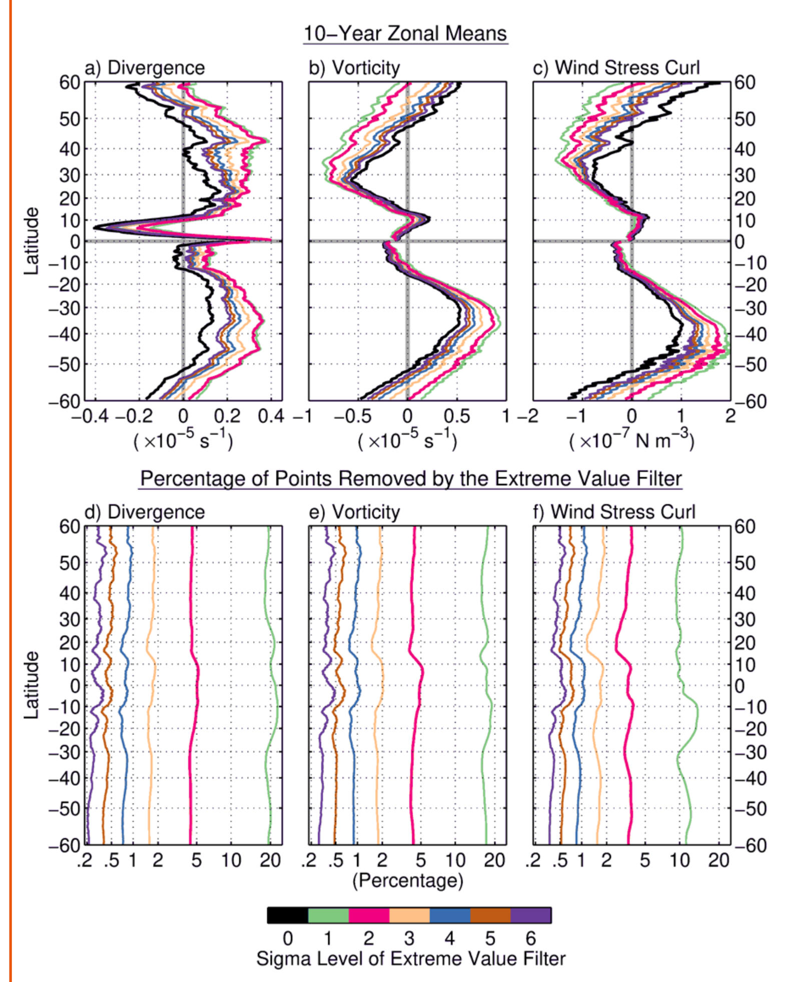

Figure 4: *(top row) Zonal mean profiles of the 10-yr mean QuikSCAT derivative wind fields as a function of latitude: (a) divergence; (b) vorticity; and (c) wind stress curl. Black lines represent the unfiltered means (corresponding to S=0), while the other curves show the means after application of the extreme-value filter with a σ-level S color-coded according to the colorbar below the plots. The zonal profiles include wind observations over ice-free oceans. (bottom row) Percentage of observations removed by the extreme value filter as a function of latitude for various choices of S as indicated by the colorbar. Note the logarithmic x-axes and Mercator projection along the y-axes.*

A value of S=2 will be used hereafter; this corresponds to a 2σ extreme value filter. The ERA-Interim has a remarkably similar zonal and time mean profiles, in both the unfiltered and 2σ filtered cases (Figure 5).

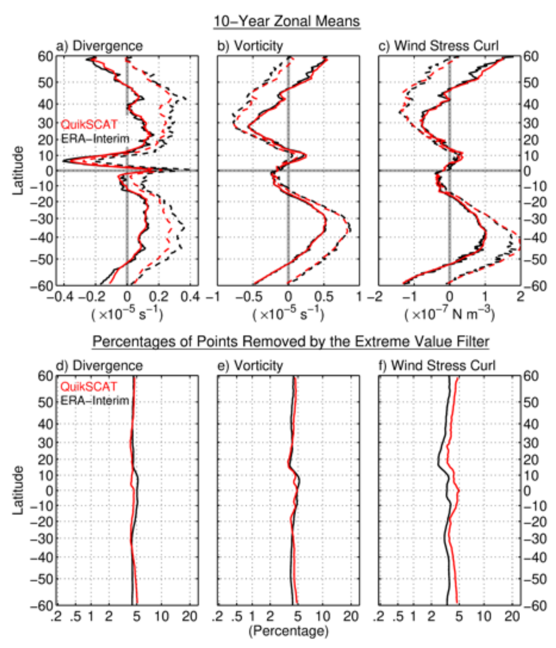

Figure 5: *Maritime zonal and time means of the QuikSCAT (red curves) and ERA-Interim (black curves) divergence, vorticity, and wind stress curl for the 10-yr period Nov 1999-Oct 2009. The solid curves in panels a-c are the full means, and the dashed curves are the 2σ filtered means.*

The zero contours in mid-latitudes contract poleward by at least 500km in both hemispheres in the 2σ filtered fields (red contours) compared with the unfiltered fields (Fig. 6, black contours). The zero wind stress curl line in the North Pacific and Atlantic basins shift northward by more than 1000km, which implies that storms play a role for maintaining the separation of the subpolar and subtropical gyres in these basins. The case for the divergence is slightly more complicated in the unfiltered means (black contours, Fig. 6c) due to the effect of the western boundary currents on the time-mean divergence. The storm tracks tend to align closely with the strong SST gradients associated with these currents, focusing strong storm-induced convergence events along a narrow corridor. The Gulf Stream Convergence Zone is one such area with a clear signature which mostly disappears in the extreme value filtered fields (O'Neill et al 2017}. This result indicates that these fundamental wind features are much more affected by synoptic weather variability than previously thought.

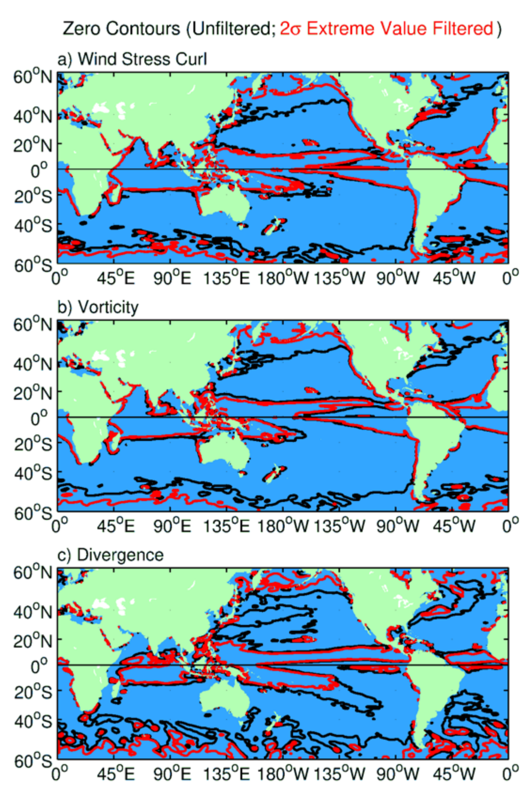

Figure 6: *Maps of the zero contours of the 10-yr mean QuikSCAT derivative wind fields. The black contours correspond to the unfiltered means, and the red contours correspond to the 2σ filtered means. For presentation purposes, the mean fields were smoothed with a two-dimensional loess smoother with half-power points of 600km zonally by 100km meridionally.*

(3) Continued

The maps below show the 10-yr mean QuikSCAT divergence, vorticity, and wind stress curl, both unfiltered (top panels) and with the 2σ filter (middle panels), as well as the difference (bottom panels). These maps highlight regional differences not apparent in the zonal mean profiles, particularly along the western boundary currents and their extensions. Air-sea interaction processes are difficult to isolate in the mid-latitudes from the much stronger signals associated with synoptic weather variability.

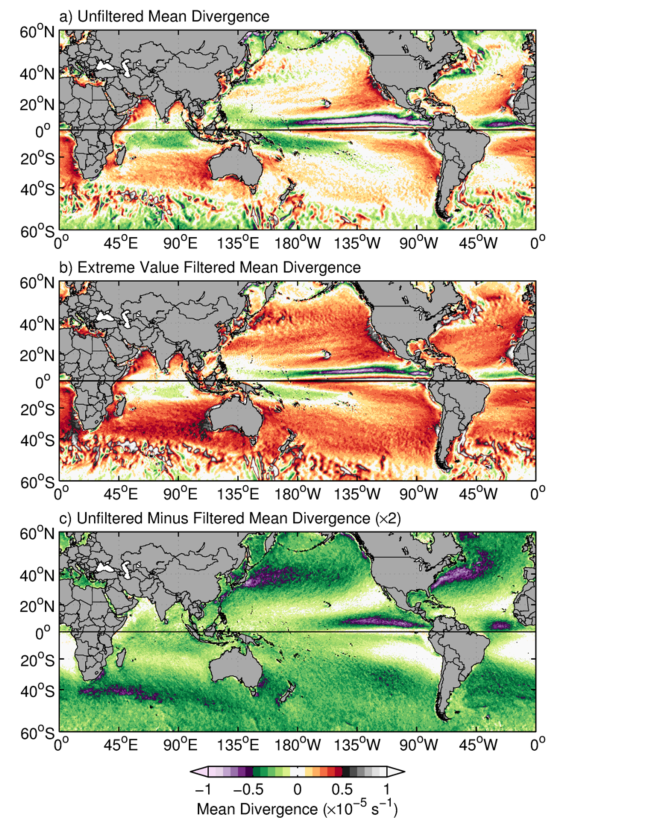

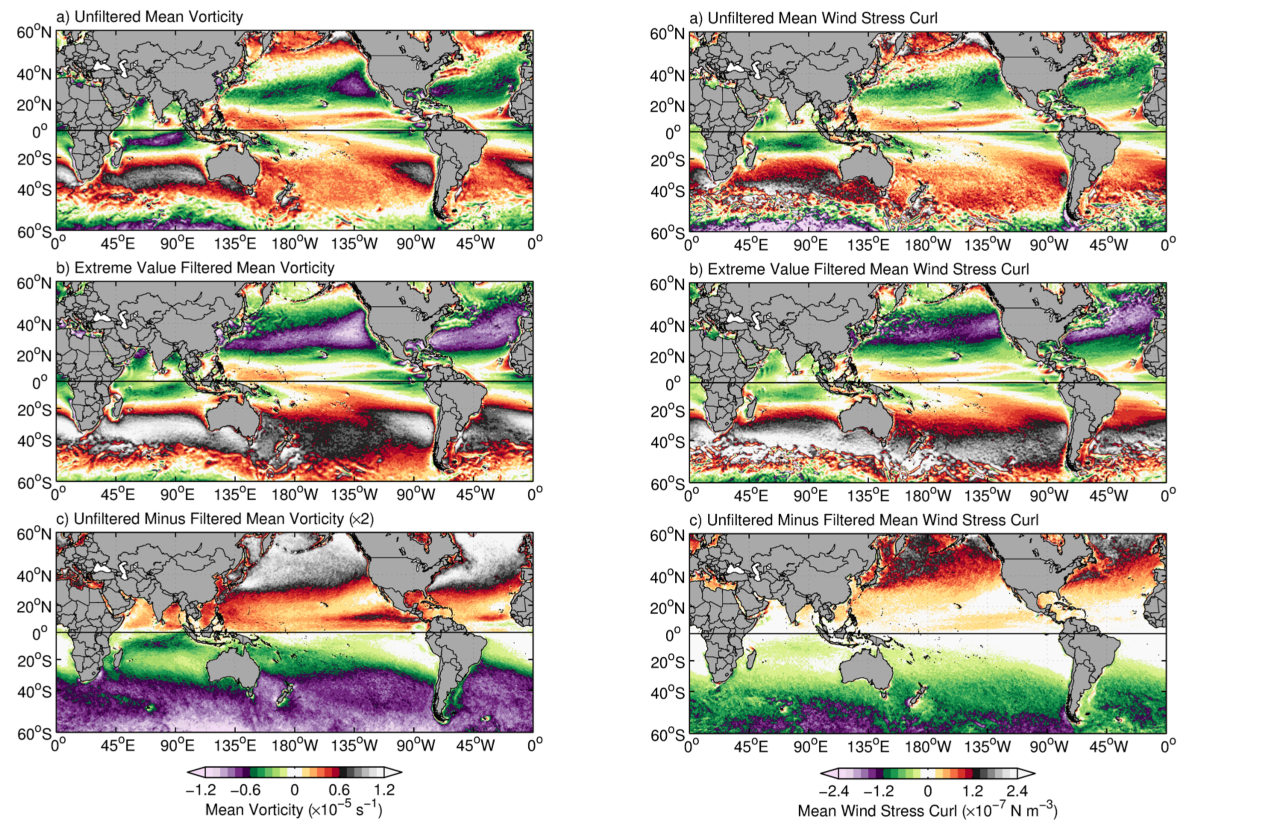

(4) Key Conclusions

1) Mid-latitude storm events generate divergence, vorticity, and wind stress curl anomalies more than 1-2 orders of magnitude greater than the climatological mean.
2) These extreme events are skewed toward cyclonic and convergent winds.
3) Extreme storm events are key to producing large-scale cyclonic wind stress curl and convergence in the climatological surface wind field in the mid-latitudes. Removing fewer than 5% of extreme events shifts the zero wind stress curl and divergence contours poleward by more than 500-1000 km
4) Relatively few synoptic scale weather events account for dynamically important large-scale features in the global wind field. Since the large-scale ocean response to wind forcing on the short timescales of synoptic weather events is weak, these results have important implications for understanding the maintenance of the large-scale wind-driven ocean circulation, which is generally thought to be driven primarily by low frequency wind variability.
5) It is difficult to separate the signature of air-sea coupling processes in the surface wind fields from synoptic-scale variability in the mid-latitude storm tracks.

(5) References

Kilpatrick, T. J., and S.-P. Xie, 2016: Circumventing rain-related errors in scatterometer wind observations. *J. Geophys. Res.*, **121**, 9422–9440

Masunaga, R., H. Nakamura, B. Taguchi, and T. Miyasaka, 2020: Processes shaping the frontal-scale time-mean surface wind convergence patterns around the Kuroshio Extension in winter. *J. Climate*, **33**, 3-25.

Milliff, R. F. and J. Morzel, 2001: The global distribution of the time-average wind stress curl from NSCAT. *Journal and Atmospheric Sciences*, **58**, 109–131.

Milliff, R. F., J. Morzel, D. B. Chelton, and M. H. Freilich, 2004: Wind stress curl and wind stress divergence biases from rain effects on QSCAT surface wind retrievals. *J. Atmos. Ocean. Technol.*, **21**, 1216–1231 .

O'Neill, L. W., T. Haack, D. B. Chelton, and E. Skyllingstad, 2017: The Gulf Stream Convergence Zone in the Time-Mean Winds. *Journal of Atmospheric Sciences*, **74**, 2383-2412, doi: 10.1175/JAS-D-16-0213.1.

O'Neill, L. W., T. Haack, and T. Durland, 2015: Estimation of time-averaged surface divergence and vorticity from satellite ocean vector winds. *J. Climate*, **28**, 7596–7620.

O'Neill, L. W., R. F. Milliff, and D. B. Chelton 2022: Extratropical Storms Fundamentally Shape the Maritime Surface Wind Climatology. *Submitted to NPJ Climate and Atmospheric Science*.

Parfitt, R., and H. Seo, 2018: A new framework for near-surface wind convergence over the Kuroshio Extension and Gulf Stream in wintertime: The role of atmospheric fronts. *Geophys. Res. Lett.*, **45**, 9909-9918.